MECHANICAL STRESS INDUCED EFFECTS FOR THE CHARACTERIZATION OF LARGE AREA SOLAR CELLS

A. Schütt, J. Carstensen, G. Popkirov, and H. Föll
Institute for General Materials Science, Faculty of Engineering, Christian-Albrechts-University of Kiel,
Kaiserstr. 2, 24143 Kiel, Germany, email: jc@tf.uni-kiel.de, Phone: (+49) 431 880 6181, Fax: (+49) 431 880 6178

ABSTRACT: CELLO measurements using a deep penetration laser (934 nm wavelength, 50 µm penetration depth) showed regions with significantly increased phase shift not visible in the corresponding phase shift map of a red laser. These regions show a significantly reduced photo current only for the deep penetrating lasers. Series of CELLO measurements on locally mechanical stressed solar cells (e.g. by bending the cell) show that especially the phase shift of the short circuit current is sensitive to stress. These strongly hint that the above mentioned structures are related to process induced stress in the solar cell. A model is discussed, where mechanical stress induced wavelength dependent changes in the laser penetration depth are related to strain induced changes of the silicon band gap. This allows for a complete fit of 16 CELLO maps to generate local data of the relative change in the band gap as a measure for local stress. Corresponding results have been found on nearly all mono- and mc-Si solar cells thinner than 250 µm, but are more pronounced on mono-Si cells. Several examples will be presented.

Keywords: Absorption, Characterization, Defects

1 INTRODUCTION

Fig. 1 depicts a simple experiment: a 180 µm thick standard mono-Si solar cell is placed on top of a standard vacuum chuck. A 50 µm thick circular Aluminum plate is positioned between chuck and cell and the vacuum switched on, establishing good electrical contact between cell and chuck. Fig. 1 a) (side view) schematically shows areas of compressive stress (red arrows) and tensile stress (blue arrows). Fig. 1 b) shows the difference in a CELLO phase shift map with and without applying vacuum which strongly hints that such stress fields are visualized. This would allow for an easy non destructive stress analysis on fully manufactured solar cells which is not easy otherwise.

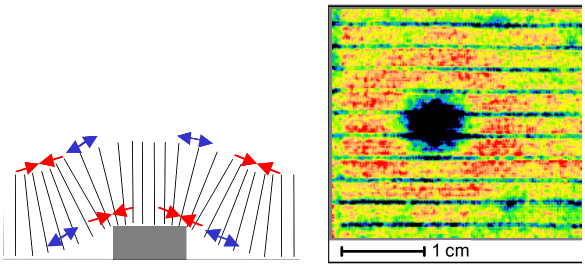

a) b)

Fig. 1: a) Side view: Al plate (gray) positioned between solar cell and a vacuum chuck (more details cf. text). b) Map of corresponding tensile stress (dark) and compressive stress (blue) extracted from CELLO measurements.

2 THEORY

Using the solution of the standard diffusion equation [1] short circuit currents can easily be calculated for light with a certain wavelength λ. As discussed e.g. in [2, 3] the linear response for a modulated intensity of the laser intensity can be easily taken into account by introducing a frequency dependent diffusion length

$$\frac{1}{L(\omega)} = \frac{1}{\sqrt{D}}\sqrt{\frac{1}{\tau} + i\omega} \qquad (1)$$

into the static solution. For $\omega \to 0$ Eq. (1) simplifies to the well known $L = \sqrt{D\tau}$. Here D is the diffusion coefficient which is related to the minority mobility μ by the Einstein relation $D = \mu kT/e$ and τ is the bulk life time; further parameters which have to be known are the surface recombination velocity at the back side of the solar cell S_b, the wavelength dependent penetration depth of light in Si $d(\lambda)$, the reflectivity, and the cell thickness d_w. For analyzing CELLO measurements the angular frequency dependent results are essential for two reasons:

- To improve the signal to noise ratio CELLO measurements are performed as Lock-in measurements of sinusodially intensity modulated laser beams.
- For solar cells with a large diffusion length L it is nearly impossible to separate D and τ only from the static solution.

When modulating the intensity to a large extend the additional information is extracted from the phase shift

$$\varphi(\omega) = \omega \Delta t(\omega) \qquad (2)$$

where $\Delta t(\omega)$ summarizes all time delays between the light intensity signal and the short circuit current, i.e. bulk life time τ, RC time constant, and diffusion delay time between generation and reaching the pn-junction

$$\Delta t_{diffusion} \approx \frac{d(\lambda)}{v} \propto \frac{d(\lambda)}{\mu} \quad ; \qquad (3)$$

here v is the average velocity of the minority carriers. Eq. (3) summarizes semi quantitatively the parameter dependence for the phase shift; having a large penetration depth of the light $\Delta t_{diffuison}$ and thus the phase shift becomes large. Increasing the mobility $\Delta t_{diffusion}$ and thus the phase shift becomes smaller; the change for different light wavelengths roughly scales with the penetration depth of the light. To analyze stress induced effects as illustrated in Fig. 1b) of course the well known dependence of the mobility on mechanical stress [4] should be considered. But a second effect related to the wavelength dependent penetration depth of light is described in the literature as well [5, 6]:

$$\alpha(\lambda)=\frac{1}{d(\lambda)}=\frac{A}{1-\exp\left(\frac{-E_{ph}}{kT}\right)}\left[\frac{hc}{\lambda}-E_g-E_{ph}\right]^2 + \frac{A}{\exp\left(\frac{-E_{ph}}{kT}\right)-1}\left[\frac{hc}{\lambda}-E_g+E_{ph}\right]^2 . \quad (4)$$

Here hc/λ is taken for the energy of the light; E_{ph} is the (average) energy of the light generated photons in the indirect band gap material; E_g is the band gap, and A a constant typically extracted from a fit to measured $\alpha(\lambda)$ curves. E_g is well known to change when applying stress. A change in E_g will lead to a change in the penetration depth $d(\lambda)$ according to Eq. (4). For a wavelength near the absorption limit of silicon this can lead to changes larger than one order of magnitude while for e.g. red visible light the stress dependence is completely negligible, leading to an extremely non linear change in the phase shift of short circuit current. This is in strong contrast to a stress induced mobility effect which as stated above shows a nearly linear change in phase shift with penetration depth. Introducing E_g as one additional fitting parameter stress dependent changes of the penetration depth for all wavelengths of light can be calculated. Incorporating these penetration depths into the fitting procedure for the short circuit current (amplitude and phase shift) as described e.g. in detail in [2, 3] additionally local mechanical stress related effects can be analyzed.

3 EXPERIMENTS, RESULTS, AND DISCUSSION

The CELLO setup uses a four probe arrangement; a laser beam of sinusodial modulated light intensity is scanned across the solar cell by a piezo-electric mirror. The short circuit current is measured using an active feedback control to ensure potentiostatic conditions to be 0 mV. Taking benefit of an FFT-algorithm and the linearity of the diffusion equation 4 frequencies are applied simultaneously to 2 lasers allowing to measure 8 maps (amplitude and phase shift for each of the 4 frequencies) in one scan. Three different lasers with wavelengths of 650 nm, 830 nm, and 934 nm have been used for the analysis (for further information cf. [2, 3, 7, 8]). A water cooled (25°C) vacuum chuck was used for contacting the back side of the solar cell.

3.1 Qualitative Analysis

CELLO phase shift maps of a mono-Si solar cell (180 µm wafer thickness) are presented in Fig. 2 using a laser light wavelength of (a) 650 nm, (b) 830 nm, and (c) 934 nm at 6 kHz. An Al stripe had been placed between the Cu plate back electrode and the solar cell as indicated by the violet line.

The Al stripe is not visible at 650 nm, slightly visible at 830 nm, and very clearly visible at 934 nm. Without the Al stripe the marked area shows no significant variation. A large number of tests has been performed to rule out that artificial effects related to the Al stripe are measured: e.g. pure geometrical effects like changing the angular dependence of the incident laser beam, changes of the reflectivity of the back side, and a change of the local electrical contact could be ruled out. Similar to Fig. 1b) the central area of increased phase shift is surrounded by an area of decreased phase shift suggesting that areas of compressive and tensile stress may be seen. The penetration depths for the three lasers are roughly 4 µm, 20 µm, 60 µm; a closer look on the quantitative phase shifts shows that the variation due to the Al stripe is much stronger than a linear dependence with the penetration depth which is a strong hint that the phase shift variation are not dominated by stress induced mobility changes.

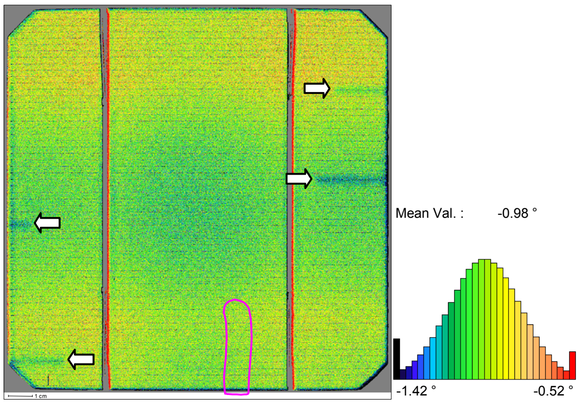

a)

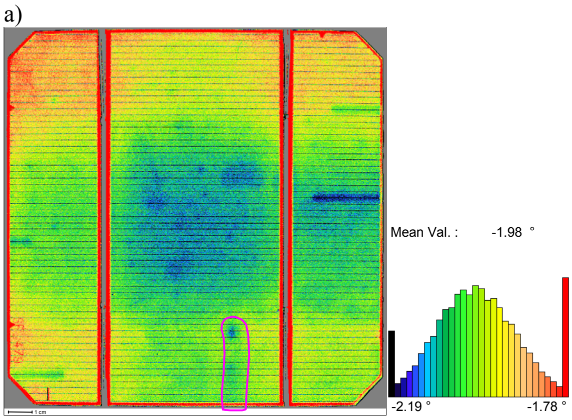

b)

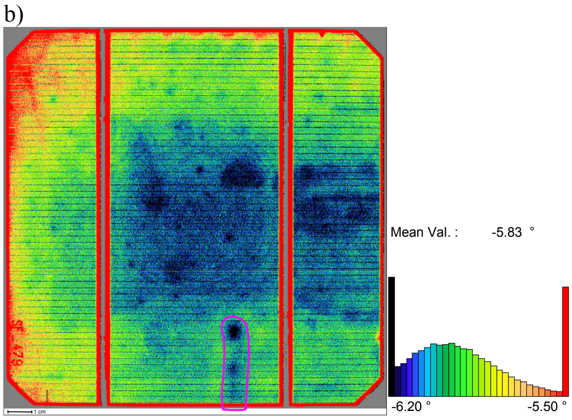

c)

Fig. 2: Phase shift dependence on laser penetration depth. a) 650 nm, b) 830 nm, c) 934 nm. The violet line indicates the position of a 50 µm thick Al stripe placed between cell and Cu back electrode. Increased serial resistances are clearly visible at broken grid fingers in a). Since no increased phase shifts are visible in Fig. a) in the marked area of the Al stripe, ohmic losses can be ruled out for the effects seen in b) and c).

Fig 3a) and 3b) show the amplitude and phase shift map of the same solar cell as in Fig. 2 without Al stripe and rotated 180°, to rule out an angular dependence of the incident laser beam. The same characteristic areas of large and small phase shift are visible. The amplitude map shows much less variation. The two circles mark areas of significant current losses. While no clear differences in the amplitude map for these areas are visible, the phase shift maps show a strongly increased phase shift for the first circle and a strongly reduced phase shift is found for the area marked by the second circle. Areas with reduced short circuit current amplitude and reduced phase shift are very common; taking into account Eq. (2) they just reflect regions with reduced effective life time. The inverse correlation of a reduced amplitude and an increased phase shift is found rarely, especially in mono-Si solar cells. It can only be understood according to Eq. (2) and Eq. (3) by a reduced local mobility or an increased local penetration depth of light. The only plausible explanation for finding a local variation in both parameters in mono-Si is intrinsic mechanical stress, i.e. stress probably induced by the back side metallization introduced while processing the solar cell. The experiments using the Al-stripe on the back side show clearly that extrinsic stress indeed results in the same finger print in the wavelength dependent short circuit current phase shift.

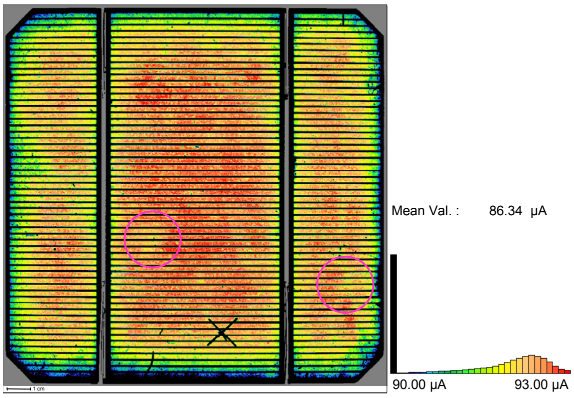

a)

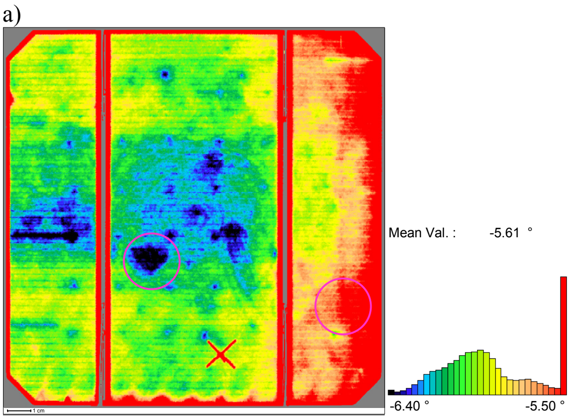

b)

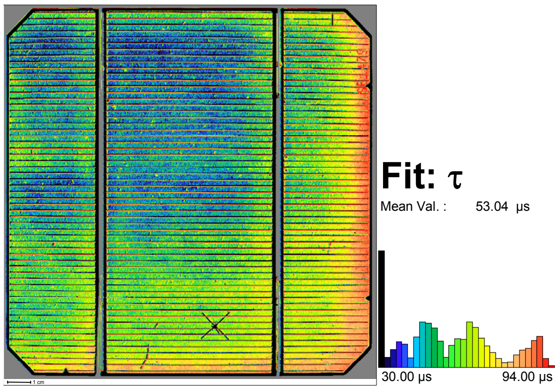

c)

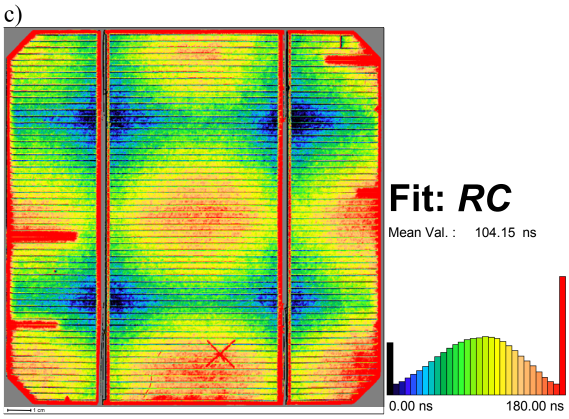

d)

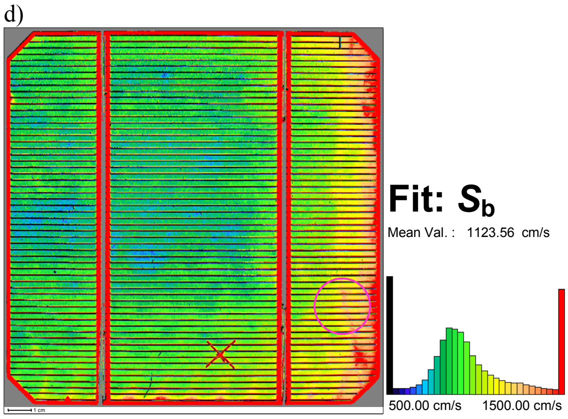

e)

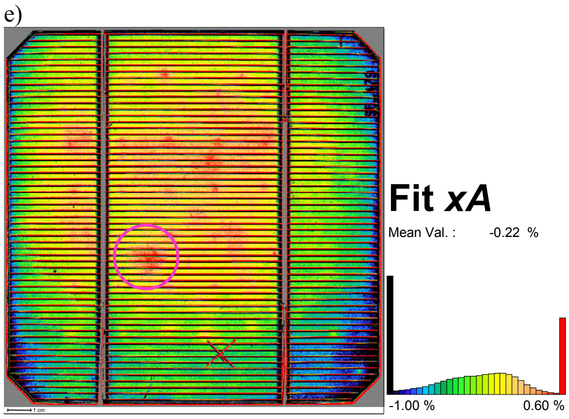

f)

Fig. 3: CELLO Data of 934 nm laser: a) amplitude, b) phase shift.
Fit results: c) τ, d) *RC*, e) $S_{b,}$, f) *xA*

3.2 Quantitative Analysis

The complete CELLO impedance analysis uses data (not all shown here) of 8 Amplitude and 8 phase shift maps of 4 different frequencies and 3 different laser wavelengths λ. A constant wafer thickness of 180 µm and a constant diffusion coefficient D of 35 cm²/s has been used for the fit. The parameters E_{ph}, A of Eq. (4) are kept constant as well, so τ, S_b, RC, and E_g are fitting parameters. Actually a scaling factor x has been introduced as a fitting parameter which describes the relative change in the band gap with respect to the non mechanically stressed case $E_g := x\, E_{g,0}$.

Fig. 3c) to 3f) show the maps of the local fitting parameters. Before focusing on the mechanical stress induced effects we will discuss the remaining fitting parameters. As can be expected for a mono-Si cell the variation in the bulk life time in Fig. 3c) is minor. The map of the RC delay time is dominated by the variation of the lateral serial resistance. The four fold symmetry related to the position of the electrodes for contacting the solar cell as well as broken grid fingers are clearly visible. These broken grid fingers already showed up as the dominant features in the phase shift map in Fig. 2a).

Fig. 3e) shows the fitting result for the surface recombination velocity at the back side of the cell. Here the systematic strong increase in the areas with missing BSF below the main bus bars and around the edges of the solar cell are nicely visible. Process induced effects at the bottom of the cell related to shading by the conveyor belt are visible as well. The right side of the cell shows significantly increased S_b. Most of the features visible as red areas with reduced phase shift in Fig. 3b) are, as expected, related to recombination losses at the back side.

Fig. 3f) shows the fitting result for the relative changes in the band gap. All areas with strongly increased phase shift in Fig. 3b) correctly show up in this map. Without taking into account the stress induced effects as described by Eq. (4) (i.e. using only the standard fitting parameters) non of the other maps showed consistent results. A second trial, taking D as a local fitting parameter, which is necessary e.g. to get correct results for UMG-Si solar cells [3], did not show consistent results for this mono cell. This is a strong hint that Eq. (4) is a (necessary and) correct implementation of the effect of mechanical stress on the short circuit currents.

3.3 Influence of the vacuum chuck

Last but not least the measurement of Fig. 1b) was repeated measuring the whole solar cell, but without any additional Al stripes or plates. Two CELLO Phase shift maps using the 940 nm laser at 6 kHz are recorded with vacuum applied to the chuck (1st map) and without vacuum (2nd map). Since the front side electrodes press the solar cell sufficiently onto the chuck, no changes in the electrical contacts and cooling of the solar cell were observed.

Calculating the difference between the two phase shift maps, several dark areas of increased phase shift difference were found as shown in Fig. 4. Each of this spots could be related to particles attached to the back side as indicated by several insets. This difference mode is sensitive only to the extrinsically induced stresses. Since for the measurements in Fig. 2 and Fig. 3 vacuum was applied to the cell, many of the dots in Fig. 4 are found here as well, while the large areas with increased phase shift are not influenced by applying the vacuum. Such measurements have been repeated on this cell several times within the last year. No relaxation of the intrinsic stress has been found.

The same differential phase shift procedure with Al stripes and plates (50 µm thickness) has been tested on various solar cell types of different Si materials and thicknesses. The effects due to tensile and compressive stress similar to Fig. 1b have been found for all tested cells up to 230 µm thickness, although they are most pronounced on mono-Si solar cells and become stronger on thinner cells. Fig. 5 shows an example for a 230 µm thick mc-Si solar cell.

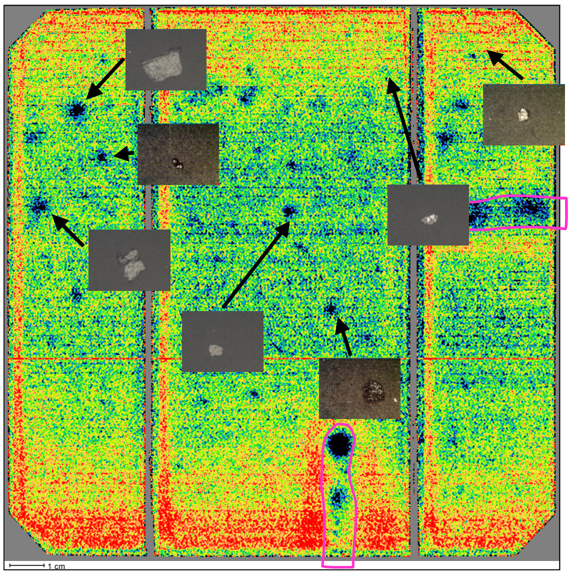

Fig. 4: Difference in Phase Shift with / without vacuum on chuck. Two Al stripes are placed between cell and Cu back contact plate (violet line).

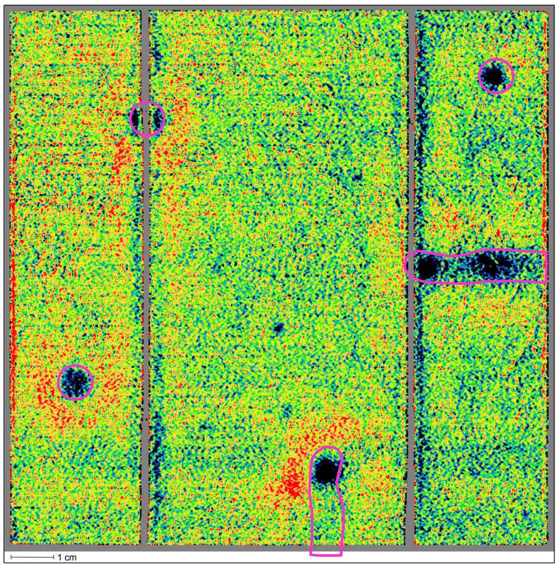

Fig. 5: Multi-Si solar cell 230 µm thick: Difference in Phase Shift with / without vacuum on chuck. Two Al stripes (violet line) and several Al plates (violet circles) are placed between cell and Cu back side contact plate

4 SUMMARY

Mechanical stress induced effects have to be considered for infrared wavelengths.

More pronounced

- thinner solar cells.
- multi and mono material.

CELLO impedance fit separates stress effects from other solar cell parameters like mobility and lifetime.

Our results show, that mechanical stress is not just a problem with respect to increased breakage of solar cells but can improve the infrared response as well.

5 ACKNOWLEDGEMENTS

We like to thank the Fraunhofer ISE in Gelsenkirchen for the supply of solar cells with various cell thicknesses.

6 REFERENCES

[1] S.M. Sze, *Physics of semiconductor devices*, Wiley & Sons, New York (1981).

[2] J. Carstensen, A. Schütt, and H. Föll, in *Proc. 24th European Photovoltaic Solar Energy Conference*, 1AO.4.5, Hamburg (2009).

[3] J. Carstensen, A. Schütt, G. Popkirov, and H. Föll, *Phys. Stat. Sol. (c)* **8(4)**, 1342 (2011).

[4] L. Garchery, I. Sagnes, P. Warren, J.-C. Dupuy, and P. Badoz, *Journal of Crystal Growth* **157**, 367-372 (1995).

[5] J. Serra, R. Gamboa, and A. Vallera, *Materials Science and Engineering B* **36**, 73 (1996).

[6] A.A. Patrin and M.I. Tarasik, *Journal of Applied Spectroscopy* **65(4)**, 598 (1998).

[7] J. Carstensen, A. Schütt, and H. Föll, in *Proc. 23rd European Photovoltaic Solar Energy Conference*, 1CV.1.38, Valencia (2008).

[8] J. Carstensen, E. Foca, S. Keipert, H. Föll, M. Leisner, and A. Cojocaru, *Phys. Stat. Sol. (a)* **205(11)**, 2485 (2008).